Available online at www.sciencedirect.com
SCIENCE DIRECT
Catalysis Today 107–108 (2005) 741–749
CATALYSIS TODAY
www.elsevier.com/locate/cattod

Molecular dynamics and solid–solid phase transformation kinetics studies of *tert*-butyl chloride confined in mesoporous silica by NQR

Griselda A. Eimer [a,*], Julio D. Fernández [a], Aldo H. Brunetti [b]

[a] *Centro de Investigación y Tecnología Química (CITeQ), Facultad Regional Córdoba, Universidad Tecnológica Nacional, CONICET, Argentina*
[b] *Facultad de Matemática, Astronomía y Física (FAMAF), Universidad Nacional de Córdoba, Ciudad Universitaria, 5000 Córdoba, CONICET, Argentina*

Available online 6 September 2005

In memory of Prof. Dr Aldo H. Brunetti.

Abstract

In this paper, we study the effect of a porous adsorbent, such as silica with a pore diameter of 375 Å on the molecular dynamics and the solid–solid phase transformations of *tert*-butyl chloride (*t*-BC) inside the pores by means of chlorine nuclear quadrupole resonance (NQR). The spin–lattice relaxation time (T_1) and the resonance frequency (ν_Q) as a function of temperature for *t*-BC, both in bulk and confined in the silica mesopores, have been measured. Changes are observed in the molecular dynamics and in the phase transition temperatures of the *t*-BC confined in the pores with respect to those corresponding to the *t*-BC in bulk. Likewise, phase transformation kinetics would seem to be altered due to restrictions of the molecular movement as a consequence of the confinement inside the porous material.

Keywords: NQR; *tert*-Butyl chloride; Silica; Phase transitions; Molecular dynamics

1. Introduction

Porous media play an important role in many aspects of science and technology. For example, mesoporous materials, such as silicas and aluminas, are of considerable importance as adsorbents and catalyst supports. Their pore architecture and chemical properties can be tailored with respect to the processing of various large and extra-large molecules depending on the chemistry behind the actual conversion. In addition, the surface of the internal pores can be modified by various post-synthesis treatments depending on the desired catalytic approach or application as adsorbents. Therefore, mesoporous silicates are regarded as an interesting model compound for the investigation of the reorientational and translational (diffusional) behavior of probe molecules with respect to the architecture and the chemical properties of the internal surface. The study of mass transport and diffusion in confined geometry is particularly important to understand catalysis when developing materials for practical applications, such as catalysts, selective adsorbents or membranes. Nuclear magnetic resonance (NMR) in particular, has become an increasingly important method for characterizing porous materials and for studying the phase behavior and molecular motion and transport of compounds confined within the porous media. So, the spin–lattice (T_1) and spin–spin (T_2) relaxation times are very sensitive to changes in the molecular environment and mobility.

It is well known that the physical properties of guest substances confined within small pores can be radically different from those of the bulk material. The dynamic and thermodynamic behavior of fluids can be strongly affected by spatial restrictions, by interactions with the pore surfaces, and by disorder introduced by the porous medium [1–11]. While the vapor–liquid transition in pores (capillary

* Corresponding author.
E-mail address: geimer@scdt.frc.utn.edu.ar (G.A. Eimer).

0920-5861/$ – see front matter © 2005 Published by Elsevier B.V.
doi:10.1016/j.cattod.2005.07.005

condensation) has been more thoroughly studied theoretically and experimentally, and is relatively well understood, the liquid–solid transition in nanopores remains largely unexplored. An understanding of melting/freezing phenomena in narrow pores is important in the fabrication of nanomaterials, in frost heaving, nanotribology, in the distribution of pollutants in soils and in the determination of pore size distributions; they are also important in many operations (e.g. adsorption and membrane separations, catalysis) in the chemical and oil industry, where meso and microporous materials are widely used.

Several studies of melting and freezing in reasonably well-characterized porous materials have been reported [12–22]. However, the general trends are unclear. First-order phase transformations have been studied by experiments on the freezing and melting of confined fluids, such as methane, carbon dioxide, oxygen, hydrogen, deuterium, argon, neon, indium and water, in several microporous and mesoporous materials, including silica glasses, zeolite Y and MCM-41 [15,17–20,22–24]. A wide range of experimental techniques have been employed in such studies, including optical techniques [15], elastic neutron scattering [17], inelastic and quasi-elastic neutron scattering [24], ac heat capacity measurements [20], differential scanning calorimetry [19], NMR signal intensity [18,23] and positronium annihilation [22]. Most reports are in general agreement on several points: a fluid confined in a nanoscale porous material exhibits a depression in its freezing point relative to that of the bulk fluid; there is hysteresis between melting and freezing, the melting temperature being higher than the freezing temperature, but still below the bulk transition and the melting and freezing transitions are continuous and broadened.

There is general agreement that the depression of the freezing point is inversely proportional to the pore diameter for a mesoporous adsorbent with unconnected cylindrical pores. This relationship derives from more than one classical thermodynamic approach and appears to fit the experimental results presented [15,18,19,23].

Explanations of the amorphous or unusual crystalline nature of the confined solid also involve the restrictive geometry of the pore, as well as the roughness of the pore wall. These factors might encourage a disordered solid to form at the walls (the contact layer), which is then propagated wholly or partly way into the confined solid [17]. Indeed, the rearrangement of the disordered solid contact layer to a more stable solid structure with a lower interfacial free energy is proposed as one possible reason for the hysteresis between freezing and melting [15,20]. Another explanation involves the initial nucleation of the solid as a sphere on cooling, which is followed by the subsequent solidification of the entire confined fluid, thus forming a cylindrical solid structure. On heating, it is the cylindrical solid, which melts, and since a cylinder has a smaller surface to volume ratio than a sphere and is thermodynamically more stable, the melting point is slightly higher than the freezing point [20]. A similar suggestion involves the presence of narrow necks between pores. Solidification is proposed to occur separately in different sections of the porous network, followed by the eventual joining of the solid crystallites through the necks, lowering the surface to volume ratio. Again, the result is a more thermodynamically stable solid, which melts at a slightly higher temperature [20].

In contrast to these studies for glasses, in which the melting temperature is decreased on confinement, some other experimental studies have found an increase in the melting temperature. For example, Klien and Kumacheva [21] reported a significant increase in the melting temperatures for two fluids (cyclohexane and octamethylcyclotetrasiloxane) confined between the mica surface of the surface force apparatus. The pore geometry is slit shaped in this case, i.e. with parallel walls. In this way, Miyahara and Gubbins [25] reported that direction and magnitude of the shift in freezing temperature in the pore is strongly dependent on the strength of the attractive forces between the adsorbate molecules and the wall, and particularly on the magnitude of these forces with respect to those between the adsorbate molecules and a wall composed of the same molecules.

A freezing mechanism has been proposed, according to which the liquid forms a layer parallel to the walls, and subsequently in-plane ordering within a layer it is accompanied by a sharpening of the layer in the transverse direction [17]. The overall properties of the adsorbed liquid change in the individual adsorbate layers. The confining walls introduce heterogeneity into the system, facilitating the layer-by-layer nucleation on freezing. In the case of weakly attractive pores, the solid begins to form at the centre of the pore, where each guest molecule undergoes the maximum interaction with other adsorbed molecules. Molecules next to the pore wall are not entirely surrounded by other molecules, and are subjected to the weaker fluid–wall interactions. Thus, phase transitions and phase behavior of the restricted substance are more strongly influenced by geometry below a certain threshold of confining pore diameter [25,26]. Support for this mechanism comes from experiments on freezing of O_2 in sol–gel glasses of different pore sizes. Crystalline order is found for larger pores, while only an amorphous phase is observed in the smaller pores [26], where the generation of microcrystallites becomes energetically unfavourable [4]. Therefore, there is a certain critical pore width below which the fluid does no show clear freezing behavior and phase transitions occur over a wider temperature range. Although numerous studies have led to a better understanding of the thermodynamic behavior of fluids within micropores, the interpretation of the results is controversial. In addition to the role of the finite-size effects, one must consider the role of the surface structure of the confining media, the heterogeneity and roughness of the surface, surface–fluid interactions and the particle size distribution of the host material.

In this project, the major topics of interest are the dynamics and phase transformations of organic substances confined in porous media. By using organic molecules forming plastic crystals as adsorbate, damage to the pore structures caused by ice formation can be avoided. An overview of the literature reflects a growing interest in the study of molecular solids formed by methyl chloromethane and their mixed crystals formed by two or more compounds of this family. *tert*-Butyl chloride (*t*-BC) has a pseudo-spherical molecular envelope and forms an orientationally disordered plastic crystalline phase as it is cooled below its freezing point. Although plastic crystals often exhibit only one solid–solid phase transition (that between the disordered and ordered phases), *t*-BC has long been known to form a partially ordered crystalline phase prior to forming the ordered phase. So, three solid phases of *t*-BC are known in the literature [27,28]. Phase I, an orientationally disordered face centered cubic phase, is obtained when the sample is cooled below its melting point (ca. 250.3 K). Phase II, tetragonal, is obtained below 213 K and remains down to 181 K where it transforms into an ordered monoclinic phase III, which becomes the low temperatures stable phase. On the basis of differential thermal analysis (DTA), in 1986 Ohtani and Hasebe [29] reported a new phase, which we will label II-OH, between 217.7 and 219.5 K. Neither other authors nor the same authors in a later NMR measurement of this compound [30] could observe the mentioned phase. We are interested in this kind of molecular solids because it can be very useful for the study of porous media, as can be observed in a recent work carried out through the NMR of *t*-BC [31] by analysing the phase transitions in this compound when the molecule is in a region of restricted movement, as is the case of fluids confined in pores, and comparing them with the bulk behavior. The presence of polymorphism in this compound makes it attractive for the study of porous media because the thermodynamic properties, and the dynamics of the guest substance confined within the host pores may be significantly different from the bulk behavior.

Nuclear quadrupole resonance (NQR) is a technique based on the interaction between the nuclear quadrupolar moment of the sensor nucleus and the electric field gradient (EFG) at the nucleus site [32]. This fact enables the use of Cl nuclei as microscopic probes for exploring the electric field prevailing in the solid. NQR is a very sensitive tool to study the structural changes of the solid and/or the molecule. In first-order phase transformations involving changes of crystal structure or molecular shape, the NQR frequency undergoes an abrupt change at the transition temperature. This variation in the NQR frequency occurs as a result of the changes of the electronic distribution within the molecules, which are affected by the intermolecular forces, and therefore it depends quite sensitively upon the environment around each molecule. When we have a disordered system, the NQR line shape becomes broadened by the static EFG distribution. When a molecule is rotating quickly, as is the case of liquids or solids with a great dynamic orientational disorder, the mean EFG leads to a null value and the NQR becomes unobservable; if the disorder is not very big, the NQR gives a very broad line that can also be unobservable.

In this work, we report the effects of physical confinement on phase transitions and molecular dynamics of *t*-BC confined in mesoporous silica using the NQR technique. Our measurements for *t*-BC in bulk were made to compare them with the behavior of *t*-BC confined in silica. We have observed the NQR signal only in phases II and III. We could not find the NQR signal in phase I probably because there is a strong orientational disorder arising from the molecular reorientation in this phase.

2. Experimental

Silica carrier (375 Å pore size and 44 m^2/g surface area) and *tert*-butyl chloride (purity p.a. >99.0%) were commercially obtained from Fluka Co. (#27706 and #19780, respectively). The silica sample was dehydrated at 400 °C under vacuum (10^{-2} Torr) for 4 h and then exposed to equilibrium vapors from liquid *t*-BC. To remove dissolved oxygen, the *t*-BC was previously degassed using the freeze-pump-thaw technique and then allowed to diffuse into the silica pores under saturated vapor pressure during 24 h at room temperature. Specific surface areas were determined by the BET method, using a Micromeritics ASAP 2000 instrument. Infrared analysis of the samples was recorded on a Jasco 5300 FT-IR spectrometer. A vacuum-heating cell with CaF_2 windows is used in our laboratory to measure IR absorption spectra of self-supporting dehydrated and non-dehydrated silica and silica plus adsorbed *t*-BC wafers (≈8 mg/cm^2). The spectra of non-dehydrated silica and silica plus adsorbed *t*-BC films were recorded in air at room temperature. The spectrum of dehydrated silica film was recorded after the sample was desorbed under vacuum for 4 h at 400 °C, and then cooled in the vacuum cell at room temperature.

To perform the measurements of NQR, both *t*-BC in bulk and *t*-BC confined in silica were sealed at vacuum in a cylindrical glass container to avoid sample hydration.

The probe head was placed inside a temperature controlled thermal bath. We used a homemade temperature control device, covering the range 77–400 K, which consisted of four coaxial and partially insulated (with aluminum oxide powder) copper cylinders immersed in a liquid N_2 bath. The temperature control was effectively achieved by heating an inner cylinder with an electronically driven heater. The temperature control was made with copper-constantan thermocouple and a Eurotherm 2604 controller. The temperature of the sample was kept constant within 0.1 K during measurement. All changes in sample temperature were achieved as slowly as possible to prevent the occurrence of the sample internal strain, which might diminish the signal-to-noise ratio.

We also made use of a pulsed, broadband, fully computerized controlled, homemade NQR spectrometer equipped with a HP8656B frequency synthesizer, an AR 150LA transmitter, a MATEC 625 receiver with a MATEC 253 preamplifier. Data acquisition was accomplished with a Waag II data acquisition ISA Board of Markenrich. The control and automatic measurement computer program was developed in our laboratory. ν_Q values were obtained within 100 Hz by fitting the FFT of the FID and looking for its maximum; a PeakFit V4 software was used to find the central frequency and the line width. T_1 values were determined within a 3% by fitting around 25 data points of the relaxation function $S(\tau)$ in a $\pi/2$-τ-$\pi/2$ two-pulse sequence as follows: 20 data points with a pulse interval τ from 0.1 to $3T_1$, and then 5 or 6 more points in the $3T_1$ to $6T_1$ interval. The thermal stability of the samples was controlled, and in addition no change in $S(6T_1)$ was observed during the measurements. The bad readings in which this value changed during the measurement interval were rejected.

3. Results and discussion

A FT-IR study of preheated silica, silica without previous heating and dehydrated silica plus adsorbed *t*-BC allowed us to evaluate the efficiency of our dehydration and organic molecules adsorption procedures. Fig. 1 shows the infrared spectra of the silica used in this study at room temperature (under line) and preheated at 400 °C for 4 h under vacuum (upper line), in the region of 2900–3800 cm^{-1}. A band at 3750 cm^{-1} attributed to hydroxyl species due to silanol groups [33] became sharp when the sample was heated at 400 °C under vacuum. Such band appeared almost completely blocked at room temperature by the presence

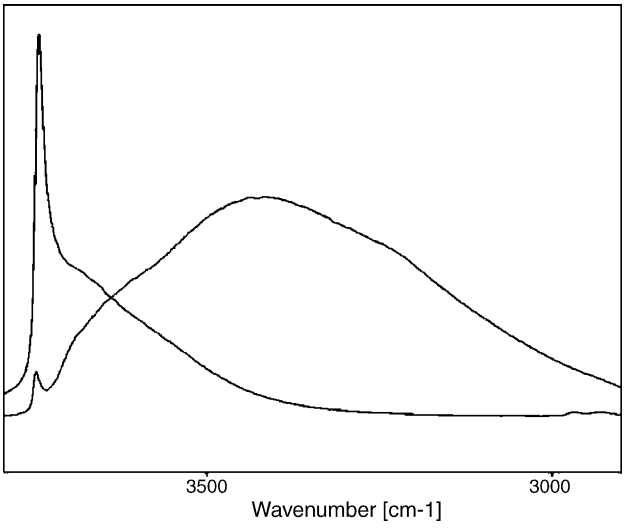

Fig. 1. Infrared spectra in the 2900–3800 cm^{-1} range of silica at room temperature (under line) and preheated at 400 °C for 4 h under vacuum (upper line).

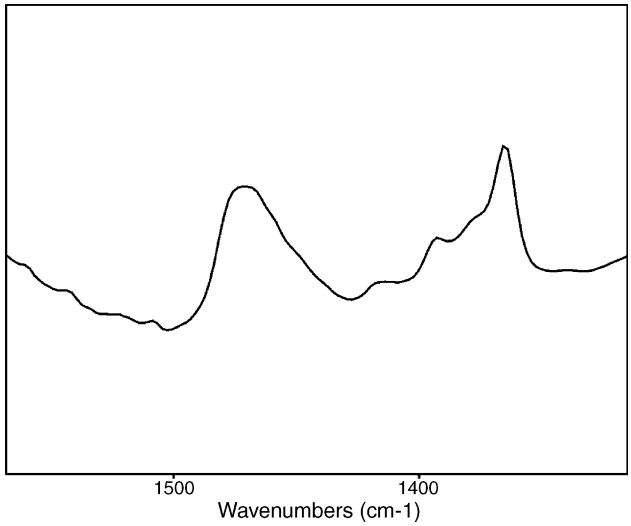

Fig. 2. Infrared spectrum in the 1300–1600 cm^{-1} range of the silica after *t*-BC adsorption at room temperature.

of water molecules physically adsorbed onto the material. In this manner, as can be observed water is completely desorbed from the sample during this previous dehydration thermal treatment. The infrared spectrum of the silica after *t*-BC adsorption in the region of 1300–1600 cm^{-1} is shown in Fig. 2. As can be seen, the sample presents absorption bands around 1470 and 1366 cm^{-1} corresponding to asymmetric and symmetric C–H stretching vibrations of the methyl groups of the *t*-BC molecules. This feature confirms the presence of *t*-BC confined in the silica and also verifies that our organic compound adsorption method is adequate.

Using Gutowsky and McCall results [34], we easily found the NQR signal in phase III of *t*-BC in bulk at 90 K. The spectrum of NQR consists of only one signal, which indicates that the two molecules in the crystalline cell ($Z = 2$) [27] are chemically equivalent. The spin–lattice relaxation time at this temperature is very short (around 60 ms).

We could follow $\nu_Q(T)$ by heating the sample in bulk until it reached 186 K, in complete agreement with Gutowsky and McCall [34]. A normal NQR behavior in molecular crystals was observed; $\nu_Q(T)$ was a monotonous function decreasing with temperature, which originated from the EFG averaging arising from the molecular movements. Gutowsky and McCall [34] report that the NQR signal disappears at 186 K as a result of a fade out which arises from a strong molecular reorientation. Since we already knew the existence of a solid–solid phase change at this temperature [27,28], we could find the signal again at a smaller frequency shifted down 350 kHz, which corresponds to phase II of the sample, and we could follow it until the temperature reached 219 K, where the sample changed to phase I. Although we looked for the NQR signal in phase I in a range of 2 MHz around the resonance frequency of phase II, we failed to observe it. Phase II-OH reported by Ohtani and Hasebe [29] was not observed. They report the existence of this phase in the range

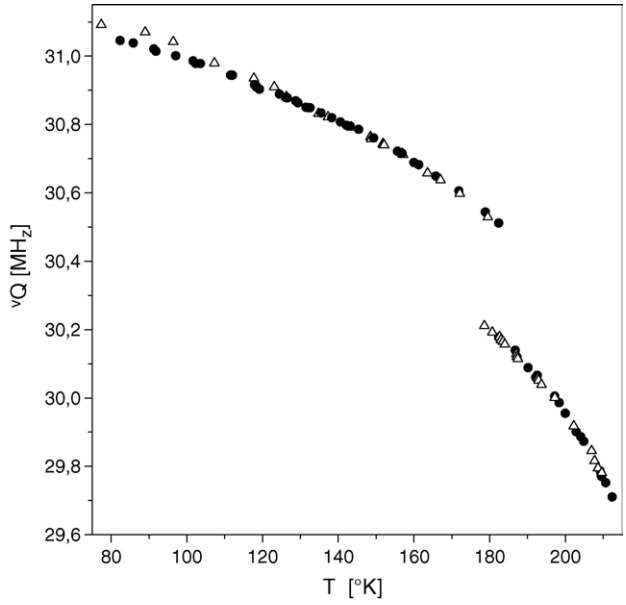

Fig. 3. $\nu_Q(T)$ of *t*-BC in bulk and confined in silica, when the sample was slowly cooled down at room temperature. "Bulk *t*-BC" is represented by circles and "confined *t*-BC" is represented by triangles.

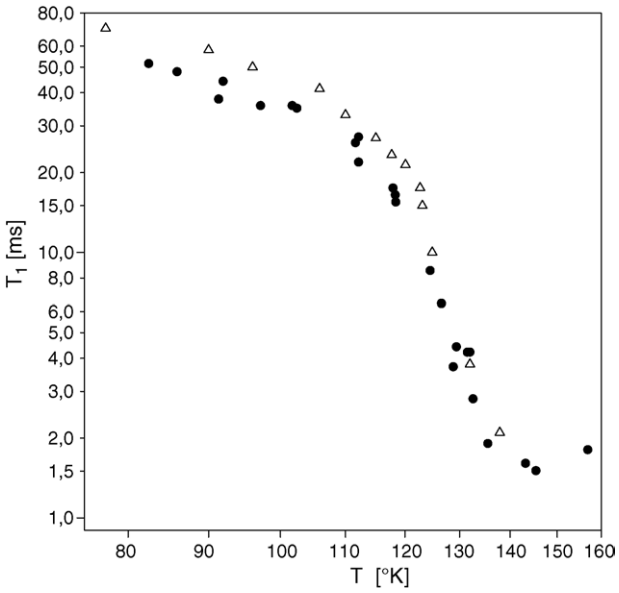

Fig. 4. $T_1(T)$ in phase III for *t*-BC in bulk and confined to silica. "Bulk *t*-BC" is represented by circles and "confined *t*-BC" is represented by triangles.

of 217.7 and 219.5 K; nevertheless, at this temperature range, we only observed the spectra of phase II without any change.

When the bulk sample was very slowly cooled down (0.5 K/min) at room temperature, we observed a similar behavior of $\nu_Q(T)$. Phase transition I–II occurs at 213.3 K, with a thermal hysteresis of approximately 5 K; the phase change is observed by the sudden appearance of the NQR signal in phase II. Phase transition II–III occurs at 182.5 K, with a thermal hysteresis of 3.5 K. We did not observe any changes neither in ν_Q(T) nor in the line width as would be observed if the II-OH phase is present. The observed thermal hysteresis is typical of first-order phase transformations.

The measured ν_Q versus temperature of *t*-BC in bulk and confined to silica when the sample was slowly cooled down at room temperature, and the temperature regions corresponding to phases II and III are shown in Fig. 3. The temperature dependence of ν_Q for *t*-BC confined in silica is different from that in the bulk, indicating a different molecular motion. At low temperatures, the frequency of resonance for the sample confined in silica mesopores is something greater than for bulk sample. Moreover, it is possible to observe that confinement of *t*-BC to silica depresses the phase transition temperatures by near 5 K. Wasyluk et al. [31] studied the molecular dynamics of *t*-BC confined in the molecular sieve MCM-41 with pore diameter of 23 Å by NMR. They reported that the temperatures of phase transitions of *t*-BC confined in this molecular sieve were depressed by near 13 K in comparison with bulk *t*-BC. Taking into account that the pore diameter of silica used in our study is 375 Å, we could corroborate that the shift in the transition temperature was inversely proportional to pore size [26]. According to Maddox and Gubbins [26], such depression of the phase transition temperatures in restricted media can be explained assuming that the critical nucleus size required for transition phase at the normal bulk transformation temperature is larger than the space allowed by the host, so that phase transition can occur only when the temperature is sufficiently low for the critical nucleus size to be smaller than the pore size.

Fig. 4 shows the measured $T_1(T)$ in phase III for *t*-BC both in bulk and confined to silica. We could only measure T_1 in phase III of the sample because it becomes very small for temperatures above 150 K. For $T > 150$ K in phase II, the value of T_1 is smaller than the lower limit we could measure since an appropriate $s(t)$ curve could not be built. We observed that the 80–115 K region is precisely where the most important contribution to the nuclear spin–lattice relaxation time takes place as a consequence of the molecular librations. For $T > 120$ K, we observed that $T_1(T)$ noticeably departed from this librational behavior, and that around 150 K it probably has a minimum. In a recent work, Brunetti [35] suggested that in the 120–160 K region the major contribution to the spin–lattice nuclear relaxation arises from thermally activated reorientations of the methyl groups around symmetry axis C_3. Furthermore, it can be observed that the values of T_1 are slightly increased when *t*-BC is confined in silica mesopores indicating that confinement restricts such molecular reorientations and librations within the pores.

The NQR technique showed to be a useful tool in the study of solid–solid phase transformations kinetics [36]. In fact, the area contained by the NQR spectrum is proportional to the number of sensor nuclei that are in a certain phase, and there is a remarkable change in the spectrum in a solid–solid phase change; therefore, the quotient of the spectrum area in

a certain instant of time and the area of the spectrum obtained in equilibrium state of that phase is the concentration of both, the transformed and the non-transformed phase. Then, if the phase transformation is sufficiently slow to allow the performance of an NQR spectrum from each phase at various intervals of time, we will be able to follow the phase change.

In our case of *t*-BC, when changing from phases II to III, the NQR frequency changes around 350 kHz, which arises from a change in the EFG contribution from the neighbouring molecules. The spectrum of each phase consists of a single line and when the two phases coexist, the spectrum of the *t*-BC consists of two lines separated by near 350 kHz; then, they must be acquired separately in our spectrometer. So, the studies of the phase transformation kinetics were carried out in the following way: the sample was cooled down (or heated up) until its temperature was close to that of the expected phase change (around 5 K "before"). The temperature was stabilised for a lapse of about 30 min. Then, we modified the sample temperature 1 K and again the sample temperature was stabilised for around 30 min. This process was repeated to observe the possible appearance of the daughter phase; when this happened, we immediately began the phase transition study at constant temperature by obtaining a spectrum of both mother and daughter phases every minute and calculating the area enclosed by the NQR spectrum in each crystalline phase. Thus, in those phases where the NQR was observed, we could follow the time evolution of the spectrum area, which is indicative of the fraction of transformed sample.

In II ↔ III transformation, we studied both the growth of the daughter phase and the decay of the mother phase for both *t*-BC in bulk and confined in silica. The studies were performed by cooling the sample until the change II → III was obtained, and then by heating the sample until we observed that the III → II phase change was beginning.

Fig. 5 shows the time evolution of the spectra areas of phases II and III during the phase transformation II → III obtained by cooling the "bulk sample" at 182.5 K. Such transformation occurs as an isothermal process in two stages. As can be observed in Fig. 5, the time evolution of the areas along the phase change can be differentiated: (a) a first stage in which, during the first 15 min the mother phase (phase II) disappears; however, the area of the daughter phase (phase III) does not reach its fullness, but it rather reaches a plateau and (b) a second stage where the area of the daughter phase (phase III) continues increasing until it reaches its equilibrium value. The complete phase change process takes place in a time interval of approximately 35 min. The analysis of the phase transformation III → II obtained by heating the sample at 186 K, showed the same behavior. The existence of a two stage process during the phase change gives evidence that two transformation processes exist along the phase change. We suggest that these two mechanisms of the transformation could be as follows: (a) a change of the crystalline cell structure with a quick spatial reordering of the molecules with a high orientational disorder and (b) a slow orientational reordering, until the sample reaches the corresponding order of the daughter phase.

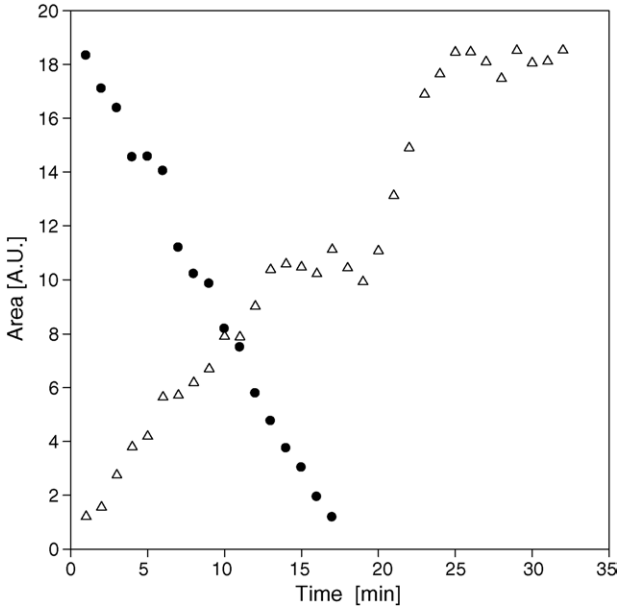

Fig. 5. Time evolution of the spectra areas in phase transformation II → III of "*t*-BC in bulk". Circles, phase II; triangles, phase III.

Fig. 6 shows the time evolution of the spectra areas of phases II and III during the phase transformation II → III obtained by cooling the "sample confined in silica" at 181.2 K. As can be observed, the mother phase (phase II) disappears during the first 90 min; however, the area of the daughter phase (phase III) does not reach its fullness, but it

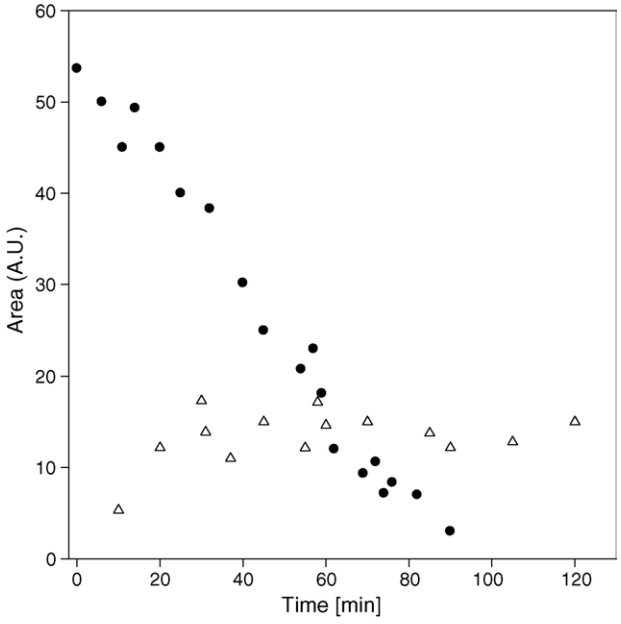

Fig. 6. Time evolution of the spectra areas in phase transformation II → III of "*t*-BC in confined in silica". Circles, phase II; triangles, phase III.

rather reaches a plateau, which is maintained even after an equilibrium time of more than 2 h. So, such phase III could reach its fullness only when the temperature was diminished to 178 K. These data show that as the sample is confined in a porous media, the phase transition is not a concerted sudden change in crystal structure but a gradual growth of phase III accompanied by a loss of phase II as the sample is slowly cooled. Moreover, the transition point is broadened since the gradual growth of phase III occurs in a range of temperature of approximately 3 K. This feature is in good agreement with the assertion that there is a certain critical pore width below which the fluid does no show a clear transition point and the phase transition occurs over a wider temperature range [4,25]. A broader range of temperature for the phase transition of *t*-BC confined in a porous media than for that of *t*-BC in bulk is also in accordance with the results reported by Hansen et al. [23]. They observed that for water in silica and MCM-41 mesopores, a solid crystallite formed in the centre of the pore at the expected depressed freezing temperature, but a fluid region rather than the usually reported amorphous solid, remained next to the pore wall until the temperature was reduced further. The freezing of this fluid contact layer occurred over a much broader range of temperatures than that of the central crystallite.

In addition, we can suppose the presence of a pretransition activity as phase II transforms to phase III in silica mesopores. Such appearance of pretransition effects accompanying the phases II–III transition would be consistent with the changes occurring at the molecular level during the transition. We believe that during the phase transition: (a) there is a transformation from the mother phase to a pretransition intermediate state that can be continued through the study of the time evolution of the volume fraction of the mother phase; (b) as soon as the phase transition begins, a new transformation process starts to take place from the pretransition region to the daughter phase, although it occurs at a smaller rate and (c) finally, when the whole mother phase is transformed, such pretransition state will remain until the temperature lowers even further. Thus, the transformation process from the pretransition heterophase to the daughter phase is only completed at a few grades below the transition temperature. It should be noted that we could not find the NQR signal of this unstable pretransition intermediate state. We believe that the intermediate state must be highly orientationally disordered, since it cannot be observed through NQR. So, we suppose that the spatial reordering would be the first process that would happen during the phase change. The crystal would turn into a heterophase pretransition region completely orientationally disordered with a crystalline structure corresponding to the daughter phase. Then, a second slower process of orientational reordering of the molecules would begin, which would be completely concluded at a slightly minor temperature. The molecular movements accompanying the phase II–phase III transition, such as spatial reordering and orientational reordering, would be strongly restricted by the confinement in the porous medium. This molecular motion can be affected both by interaction with the surface and by steric restrictions. Such feature could explain both the range of temperature observed for the phase transition of *t*-BC confined in silica and the slower phase transformation velocity for the *t*-BC confined in silica than that for *t*-BC in bulk.

On the other hand, the continuous nature of the phase transition has also been explained by Maddox and Gubbins [26] in a simple way, considering the polydispersity of the porous materials used. So, if the transition point is sharp at a specific temperature for a specific pore size, a range of pore sizes would provide a range of phase transition points.

Phase transformation III → II obtained by heating the "sample confined in silica" continues to be studied and similar results to the ones presented in this work are expected.

Fig. 7 shows the time evolution of the spectrum areas of phase II along phase transformations I → II for "*t*-BC in bulk". The phase change to phase II is observed by cooling down the sample in bulk at 213 K. It was impossible to measure the time evolution of the area of phase I during the transition because it is orientationally disordered, and therefore its NQR cannot be observed. Thus, in phase transformations I → II our study was only performed in the time evolution of phase II. As can be observed the area of the daughter phase (phase II) grows until it reaches its equilibrium value in a time period of approximately 15 min. Then, phase transformation I → II is much quicker than II → III for *t*-BC in bulk. According to thermodynamic data [27], phase transition I → II has a much lower ΔH (and ΔS) than phase transition II → III, which indicates that the major structural rearrangement occurs at the latter point.

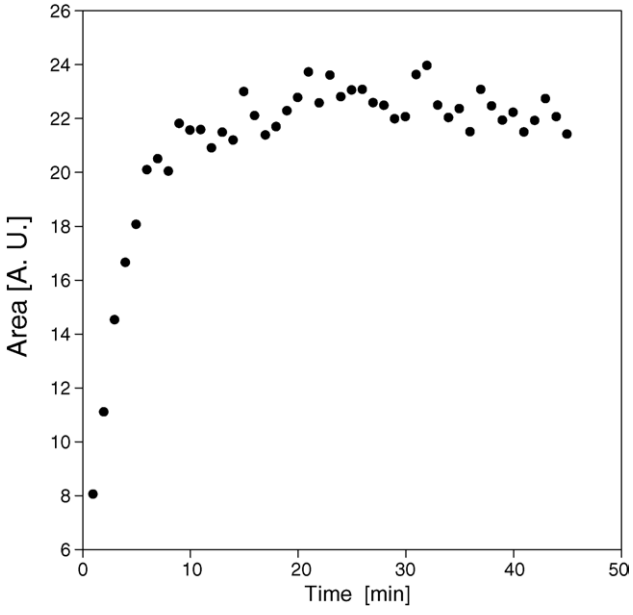

Fig. 7. Time evolution of the spectra areas in phase transformation I → II of "*t*-BC in bulk". Circles, phase II.

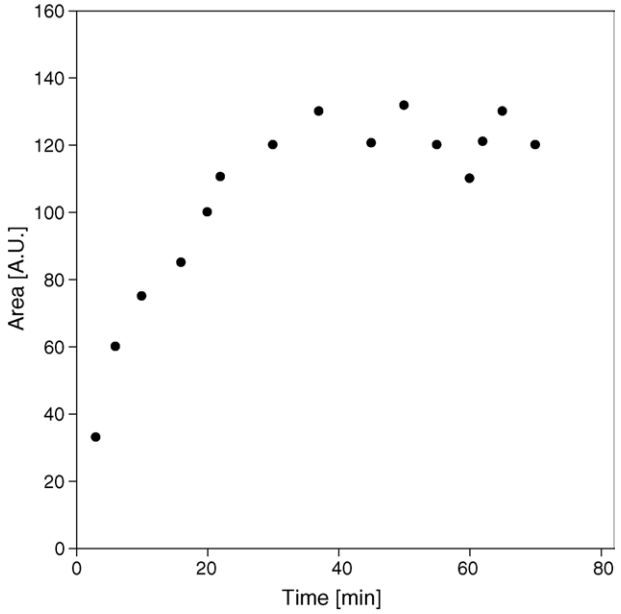

Fig. 8. Time evolution of the spectra areas in phase transformation I → II of "*t*-BC in confined in silica". Circles, phase II.

These data allow us to explain the minor time interval needed to reach the equilibrium in phase transition I → II with respect to that needed for phase transition II → III. Moreover, if we keep in mind that phase I cannot be observed by NQR, phase transformation kinetics I → II could be similar to that observed in phase change II → III, although only the second stage (the orientational reordering) could be observed, since both phase I and a supposed intermediate state are not seen by NQR.

Fig. 8 shows the time evolution of the spectrum areas of phase II along phase transformations I → II for "*t*-BC confined in silica mesopores". The phase change to phase II is observed by cooling down the sample at 208.5 K. Again, our study was only performed in the time evolution of phase II because phase I is unobservable in a NQR experiment. As can be seen, the area of the daughter phase (phase II) reaches its equilibrium value in a time interval of approximately 50 min. As we could expect, the phase transformation kinetics I → II for *t*-BC confined in silica mesopores is rather slower than that for *t*-BC in bulk. As has been mentioned, the molecular motions (spatial reorientations and orientational reorientations) involved in the phase transition would be affected by the spatial restrictions from porous medium. So, the mobility of the molecules of *t*-BC confined in the mesoporous silica and its reorientational dynamics during phase transition would be diminished by these effects of physical confinement.

4. Conclusions

We made measurements of ^{35}Cl NQR in *t*-BC both in the bulk and confined in mesoporous silica for phases II and III. The temperature dependence of ν_Q in both phases showed a normal Bayer monotonous decreasing curve. Thermal hysteresis, which is typical of first-order phase transformations, has been observed. The molecular dynamics for *t*-BC confined in silica is different from that of *t*-BC in bulk and the phase transitions temperatures of confined *t*-BC are depressed by near 5 K in comparison with bulk *t*-BC. The values of T_1 are slightly increased when *t*-BC is confined in silica mesopores, which indicates that the mobility of the molecules is restricted by the confinement within the pores.

Measurements of time evolution of the area contained by the NQR spectrum from each phase during the phase transitions allowed us to follow the phase change behavior.

Phase change II ↔ III of the *t*-BC in bulk would occur isothermally in two temporal stages. First, a quick spatial reordering of the molecules to a highly orientationally disordered intermediate state, and then a slow orientational reordering of the molecules from that intermediate state to the daughter phase. A model of this type would also explain our measurements of phase transformation I ↔ II of *t*-BC in bulk. As *t*-BC is confined in silica, we have found that phase transition II → III is broadened and occurs over a temperature range of approximately 3 K. We could suppose the existence of an orientationally disordered pretransition intermediate state, whose orientational reordering into daughter phase crystal could only be completed as the temperature is decreased a few grades below the transition temperature. The phase transformations kinetics I ↔ II and II ↔ III for *t*-BC confined in silica mesopores are rather slower than those for *t*-BC in bulk. The molecular motions involved in the phase transitions, such as positional reordering and orientational reordering, would be strongly affected both by interaction with the surface and by steric restrictions as a result of physical confinement.

In addition, the FT-IR technique allowed us to evaluate the performance of our methods for silica previous dehydration and *t*-BC adsorption in silica.

Acknowledgements

Partial financial support provided by SECYT-UNC and CONICET from Argentina is gratefully acknowledged.

References

[1] D. Awschalon, J. Warnock, Phys. Rev. B 35 (1987) 6779.
[2] D. Morineau, G. Dossech, C. Alba-Simionesco, P. Llewellyn, Philos. Mag. B 79 (1999) 1847.
[3] R. Mu, V.M. Malhotra, Phys. Rev. B 44 (1991) 4296.
[4] S. Stapf, R. Kimmich, T. Zavada, Appl. Magn. Reson. 12 (1997) 199.
[5] D. Aksnes, L. Gjerdaker, J. Mol. Struct. 475 (1999) 27.
[6] D. Aksnes, L. Gjerdaker, L. Kimtys, J. Mol. Struct. 509 (1999) 297.
[7] D. Aksnes, L. Gjerdaker, L. Kimtys, J. Mol. Struct. 522 (2000) 209.
[8] D. Aksnes, L. Gjerdaker, L. Kimtys, Appl. Magn. Reson. 18 (2000) 255.

[9] L. Gjerdaker, D. Aksnes, G. Sorland, M. Stocker, Microporous Mesoporous Mater. 42 (2001) 89.
[10] H. Booth, J. Strange, Mol. Phys. 93 (1998) 263.
[11] C. Jackson, G. McKenna, J. Chem. Phys. 93 (1990) 9002.
[12] W. Patrik, A. Kemper, J. Chem. Phys. 42 (1938) 369.
[13] G.K. Rennie, J. Clifford, J. Chem. Soc., Faraday Trans. I 73 (1977) 680.
[14] L. Tell, H. Maris, Phys. Rev. B 28 (1983) 5122.
[15] J. Warnock, D. Awschalon, M.W. Shafer, Phys. Rev. Lett. 57 (1986) 1753.
[16] H. Torii, H. Maris, G. Seidel, Phys. Rev. B 41 (1990) 7167.
[17] P. Sokol, W. Ma, K. Herwig, W. Herwig, W. Snow, Y. Wang, J. Koplik, J. Banavar, Appl. Phys. Lett. 61 (1992) 777.
[18] J. Strage, M. Rahma, E. Smith, Phys. Rev. Lett. 71 (1993) 3589.
[19] K. Unruh, T. Huber, C. Huber, Phys. Rev. B 48 (1993) 9021.
[20] E. Moltz, A. Wong, M. Chan, J. Beamish, Phys. Rev. B 48 (1993) 5741.
[21] J. Klien, E. Kumacheva, Science 269 (1995) 816.
[22] J. Duffy, N. Wilkinson, H. Fretwellm, M. Alam, R. Evans, J. Phys. Cond. Matter 7 (1995) 713.
[23] E. Hansen, M. Stoker, R. Schmidt, J. Phys. Chem. 100 (1996) 2195.
[24] K. Edler, P. Reynolds, F. Trouw, J. White, J. Chem. Soc. Chem. Commun. (1996) 155.
[25] M. Miyahara, K. Gubbins, J. Chem. Phys. 106 (1997) 2865.
[26] M. Maddox, K. Gubbins, J. Chem. Phys. 107 (1997) 9659.
[27] R. Rudman, J. Mol. Struct. 485–486 (1999) 281.
[28] J. Tamarit, D. Lopez, X. Alcobé, M. Barrio, J. Salud, L. Pardo, Chem. Mater. 12 (2000) 555.
[29] S. Ohtani, T. Hasebe, Chem. Lett. (1986) 1283.
[30] T. Hasebe, S. Ohtani, J. Chem. Soc., Faraday Trans. I 84 (1988) 187.
[31] L. Wasyluk, B. Peplinska, J. Klinowski, S. Jurga, Phys. Chem. Chem. Phys. 4 (2002) 2392.
[32] H. Chihara, N. Nakamura, in: J. Smith (Ed.), Advances in Nuclear Quadrupole Resonance, vol. 4, Heyden, London, 1981, p. 1 (Chapter 1).
[33] G. Eimer, L. Pierella, G. Monti, O. Anunziata, Catal. Lett. 78 (1–4) (2002) 65.
[34] H. Gutowsky, D.W. McCall, J. Chem. Phys. 32 (1960) 548.
[35] A. Brunetti, J. Mol. Struct. 690 (1–3) (2004) 83.
[36] C. Meriles, A. Pérez, C. Schurrer, A. Brunetti, Phys. Rev. B 56 (1997) 14374.